NASA-CR-197458

33545

33 p

AIRESEARCH MANUFACTURING COMPANY
OF CALIFORNIA

INVESTIGATION OF COMPLIANT
FOIL BEARINGS FOR LONG-LIFE
LIQUID HYDROGEN PUMPS

PHASE I INTERIM REPORT

CONTRACT NAS 1-15807

80-16884 March 21, 1980

(NASA-CR-197458) INVESTIGATION OF COMPLIANT FOIL BEARINGS FOR LONG-LIFE LIQUID HYDROGEN PUMPS Interim Report (AiResearch Mfg. Co.) 33 p

N95-70634

Unclas

Z9/37 0033545

GARRETT

AIRESEARCH MANUFACTURING COMPANY
OF CALIFORNIA

# INVESTIGATION OF COMPLIANT FOIL BEARINGS FOR LONG-LIFE LIQUID HYDROGEN PUMPS

PHASE I INTERIM REPORT

CONTRACT NAS 1-15807

80-16884 March 21, 1980

Number of pages 32

Original date March 21, 1980

Prepared by R. Brown
A. Gu

| Revision | Date | Pages Affected (Revised, Added, Eliminated) |
|---|---|---|
| | | |

FORM 23 77( 2 71

CONTENTS

ILLUSTRATIONS

## 1. PUMP OPERATIONAL REQUIREMENTS

The operational requirements of the pump are summarized in Table 26, NASA Report CR-145369. Note that this table is incorrectly labeled: the conditions listed apply to a fixed-ratio shaft-driven pump rather than to a variable-speed pump. The conditions for the variable-speed pump are given in Table 27 of the same report. As indicated in the table and in Figure 70, the pump flow rate will be controlled by throttling from 100 percent flow at takeoff (condition 4) to as low as 12.6 percent at flight idle (condition 7).

It is the off-design conditions that will generate the maximum radial loads on the pump bearings. The radial load imposed on the bearings by the pump impeller(s) is a function of the pressure rise, impeller specific speed, percentage of design flow, and the design of the collector receiving the flow from the impeller. Some potential collector designs are listed below:

(a) Volute (constant increase in flow area around the impeller)

(b) Double-volute

(c) Concentric (constant flow area around the impeller)

(d) Vaned diffuser followed by a concentric collector

Provided the pump is operating close to design flow, the volute collector imposes a very small static load on the pump bearings because the pressure at the periphery of the impeller is the same at all points around the circumference. At off-design flow, depending on the proximity of the volute cutoff to the impeller outside diameter, high static radial loads are generated. A substantial dynamic load may be superimposed on the static radial load. The static load can be minimized by use of a double-volute with outlets 180 deg apart or, in the case of two-stage pumps, the single volutes can be displaced by 180 deg. The concentric collector is not as efficient as the volute, but it has the advantage that the off-design static and dynamic radial loads are much lower.

Figure 1-1 shows the static radial thrust curves for a 2838 specific speed pump with an ordinary volute, a double-volute, and a concentric collector. The curves shown represent the magnitude of the static radial load at different flow rates. The angular direction of the load moves around the volute, depending on the percentage flow rate ($Q/Q_n$). A dynamic load rotating with the impeller must be superimposed on the static radial thrust shown. The literature usually gives the following expression for radial thrust:

$$L = K \cdot D \cdot B \cdot \Delta P \qquad (1\text{-}1)$$

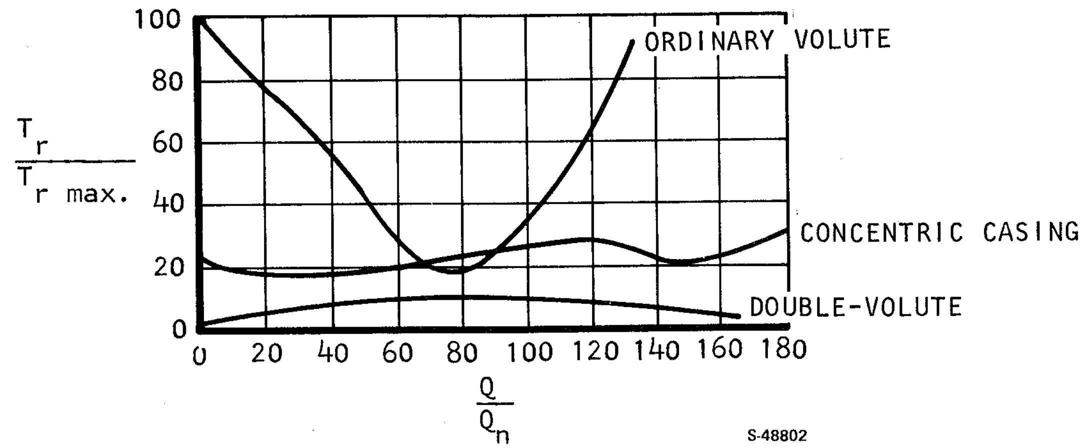


Figure 1-1. Influence of Casing Design on Radial Thrust vs Flow Rate in a Pump of Given Specific Speed

where L = radial thrust, lb

D = impeller diameter, in.

B = impeller width (over shrouds), in.

$\Delta P$ = pump pressure rise, psi

K = empirical factor

For volute pumps, K may reach 0.15 when the pumps are operating at close to zero flow.

Because the pump has to operate over a wide flow range, it was apparent early in the study that it would be necessary to minimize the steady-state loads to allow use of a foil bearing of reasonable size. With the two-stage pump described in NASA CR-145369, the two impeller outlet elements can be rotated 180 deg from each other, thereby cancelling out the steady-state loads, assuming the pressure rise across both impellers is the same. If a foil thrust bearing is used, it is advantageous to arrange the two pump impellers back-to-back (impeller inlets looking in opposite directions) instead of using the arrangement shown in CR-145369. The back-to-back arrangement balances the axial static and momentum thrust loads on the impeller, but it has the disadvantage that the transition duct from the discharge of the first impeller to the inlet of the second impeller is much more complicated. Assuming that if a foil thrust bearing is used the impellers will be arranged back-to-back, the axial thrust may be calculated from an inlet pressure of 50 psia acting over the shaft seal area of 0.19 sq in. (0.5 in. nominal sealing diameter), giving a load of 9.5 lb. Because the axial thrust can easily be taken by a ball bearing outside the liquid hydrogen environment without compromising the pump design, a foil thrust bearing is not recommended. The ball bearing has the capability of sustaining the high transient loads that may occur in the event of vaporization of hydrogen in the first impeller with the second impeller operating on liquid hydrogen.

There is no literature reporting test data on the magnitude and frequency of the dynamic radial thrust loads on pumps operating off-design, probably because the need for these kinds of data has not arisen. Normally pumps are operated close to design flow or, as in the case of engine afterburner pumps, operating life is short and bearings are substantial.

AiResearch has designed and tested an experimental centrifugal main engine fuel pump for the General Electric Company. This pump was run at flow rates from 2 to 150 gpm with discharge pressures in the range of 700 to 1050 psid at a drive speed of 27,500 rpm. Bearing loads were not measured, but dynamic discharge pressures were recorded. The data show that at 150 gpm (design flow) discharge pressure was 1050 psid, with a fluctuation of $\pm 20$ psi at a frequency corresponding to the revolutions per minute of the pump. At low flow pressure, fluctuations increased to $\pm 150$ psi.

Because the General Electric pump had a vaned diffuser followed by a concentric collector, the steady-state radial thrust was probably very small. It is also probable that the dynamic load on the pump bearing system was directly related to the magnitude of the discharge pressure fluctuations. Using these data in Eq. 1-1, the radial dynamic thrust for the $LH_2$ pump was calculated as follows:

$$L = 0.160 \times 3.73 \times 0.115 \times 698 = 48 \text{ lb} \qquad (1-2)$$

where $K$ = empirical factor = 152/950

$D$ = impeller diameter = 3.73 in.

$B$ = impeller width = 0.115 in. (two shrouds, each 0.03 in., plus 0.055-in. channel)

$P$ = 698 psid (two impellers, each 349 psid)

The estimated weight of the rotating group is 1 lb. Assuming the pressure rise is proportional to $(\text{rpm})^2$ and the operating speed to develop 698 psid is 50,000 rpm, then a general expression for the radial load can be defined

$$\text{Radial load } L = 1 + (1.92N^2 \times 10^{-8}) \text{ lb} \qquad (1-3)$$

To define the bearing loads with more confidence, a test program is proposed in para. 3.1.

A potential problem with vaned diffuser pumps is the existence of a discontinuity in the pump pressure rise versus flow curve, which makes it impossible to maintain stable flow control by throttling. This instability can be eliminated by modifying the diffuser at the expense of a somewhat lower pressure rise at design flow. Because the power required to drive the pump remains unchanged, the net result is a lower efficiency at design flow. This condition is illustrated in Figure 1-2, which shows test data on the AiResearch AWACS pump before and after diffuser rework.

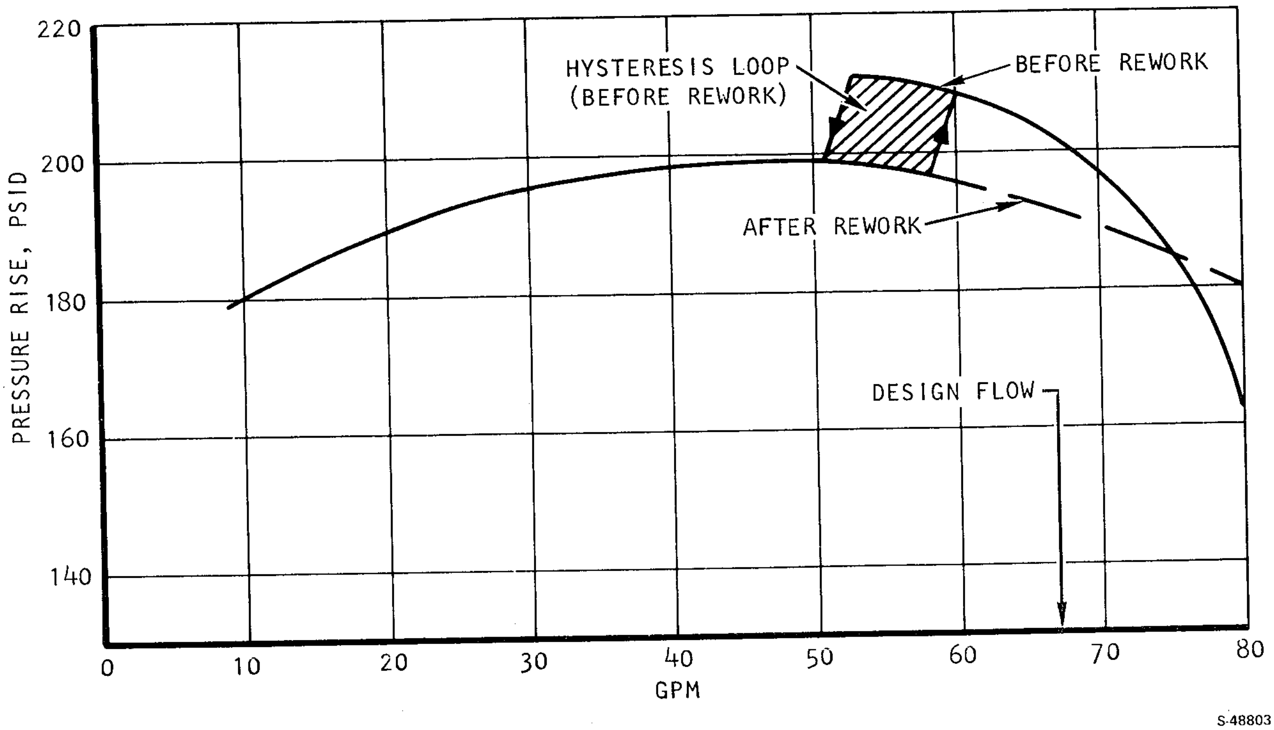


Figure 1-2. AiResearch AWACS Pump Before and After Diffuser Rework

As an alternative to controlling pump flow by throttling, a variable-area diffuser can be used. This has the advantage that off-design pressure fluctuations are much lower than those associated with the throttled fixed-area diffuser pump. Anticipating a trend toward centrifugal main engine fuel pumps on engines using conventional fuels, AiResearch built and tested a variable-area diffuser pump and demonstrated stable control over a wide flow range.

The shutter contains 12 slots of different lengths that were moved axially across the diffuser inlet, progressively closing off the diffuser ports. Shutter position was controlled automatically by comparing the output signal from a turbine type flowmeter measuring pump flow with a predetermined manually set required flow. The error signal between required and actual flow was used to energize an Abex 4-way servovalve, which repositioned the shutter by applying fuel pressure to the control piston. Shutter position was monitored with a linear motion potentiometer. Fuel supply for the servovalve was taken from the periphery of the pump impeller upstream of the shutter to ensure a relatively constant supply pressure independent of downstream impedance.

Development of a long-life $LH_2$ pump will require careful design to minimize the transfer of heat between the "wet" portion of the pump and the engine gearbox, but this is not considered a high technical risk. Aside from bearings, the only other technical risk is in the shaft seal, where risk may be directly related to the acceptable leakage rate. Evaluation of potential shaft seal designs and leakage rates can be incorporated into the bearing test program with little increase in cost if face seals instead of the labyrinths shown in Figure 3-1 are used in the bearing test rig.

## 2. BEARING DESIGN ANALYSIS

### 2.1 RELEVANT PHYSICAL PROPERTIES OF $LH_2$

To assess the feasibility of foil bearings for the $LH_2$ pump application, the first step is to compare the physical properties of $LH_2$ with air, which is the working fluid for most foil bearing applications. According to the preliminary pump design reported in NASA CR-14539, the pump pressure ranges from 50 to 735 psia and the temperature varies from 45° to 50°R. The viscosity, density, thermal conductivity, and specific heat of $LH_2$ under these conditions have been compiled and are presented in Figures 2-1 through 2-4. It is seen that $LH_2$ behaves like an incompressible fluid in the normal pump operating condition and that its viscosity is lower than that of air. These characteristics were considered in sizing bearings for the $LH_2$ pump application.

### 2.2 JOURNAL BEARINGS

The load requirement for journal bearings was first estimated. A preliminary sizing was then performed based on the load capacity and startup stability consideration. The bearing loss was also calculated.

#### 2.2.1 Journal Bearing Load

The total journal bearing load consists of three parts:

$$W_t = W_r + W_g + W_u \tag{2-1}$$

where $W_r$ = the rotor weight

$W_g$ = the gyroscopic maneuver load

$W_u$ = the maximum synchronous hydraulic radial unbalance load, which occurs at minimum off-design pump flow

The rotor weight is estimated to be 1 lb, based on the preliminary pump design. A sketch of this design is shown in Figure 2-5.

The gyroscopic load is usually small in transport aircraft. It is defined as:

$$W_g = \frac{I_p \omega \Omega}{r_e} \tag{2-2}$$

where $I_p$ = the rotor polar moment of inertia

$\omega$ = the rotor speed

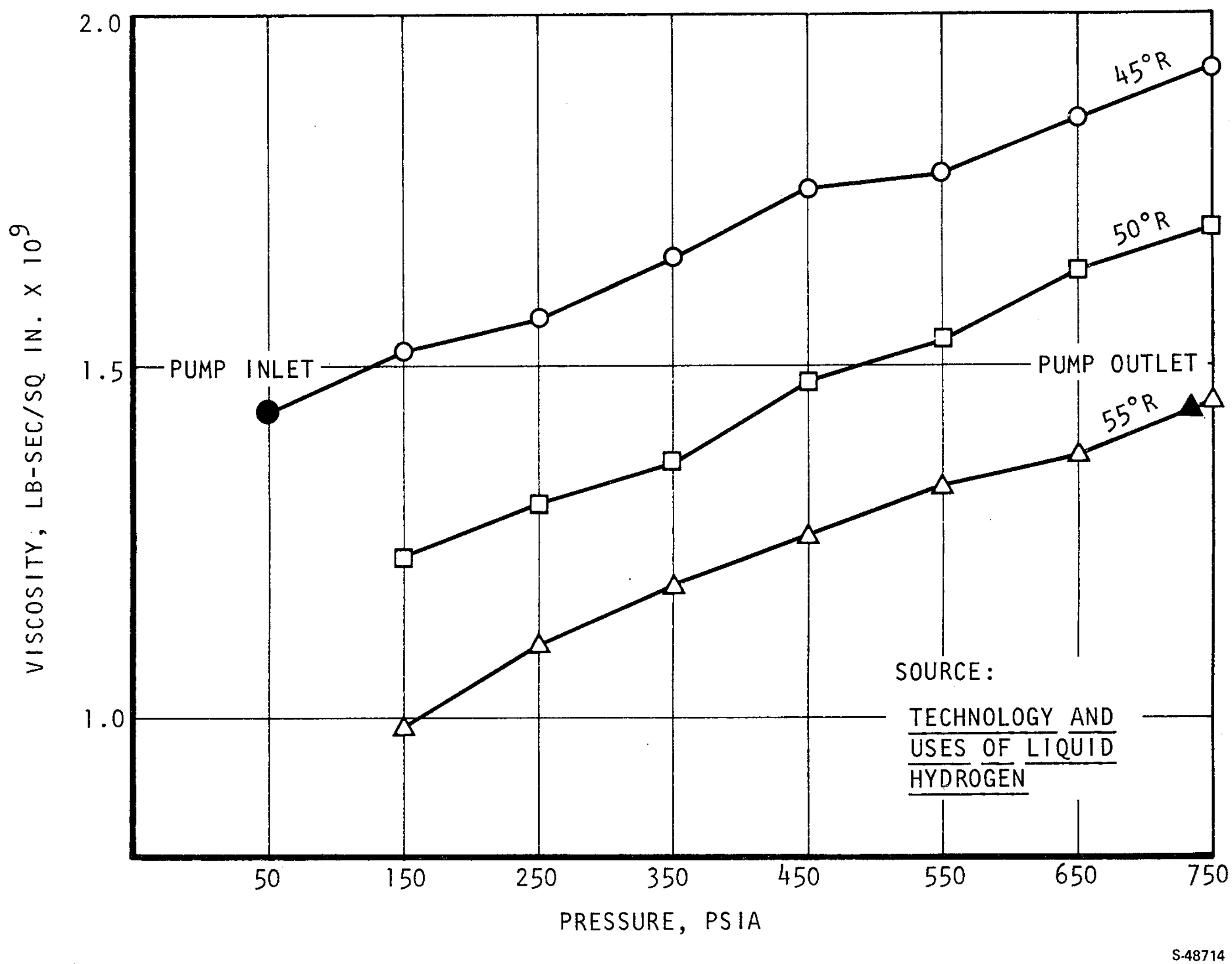


Figure 2-1. Viscosity vs Pressure for Hydrogen

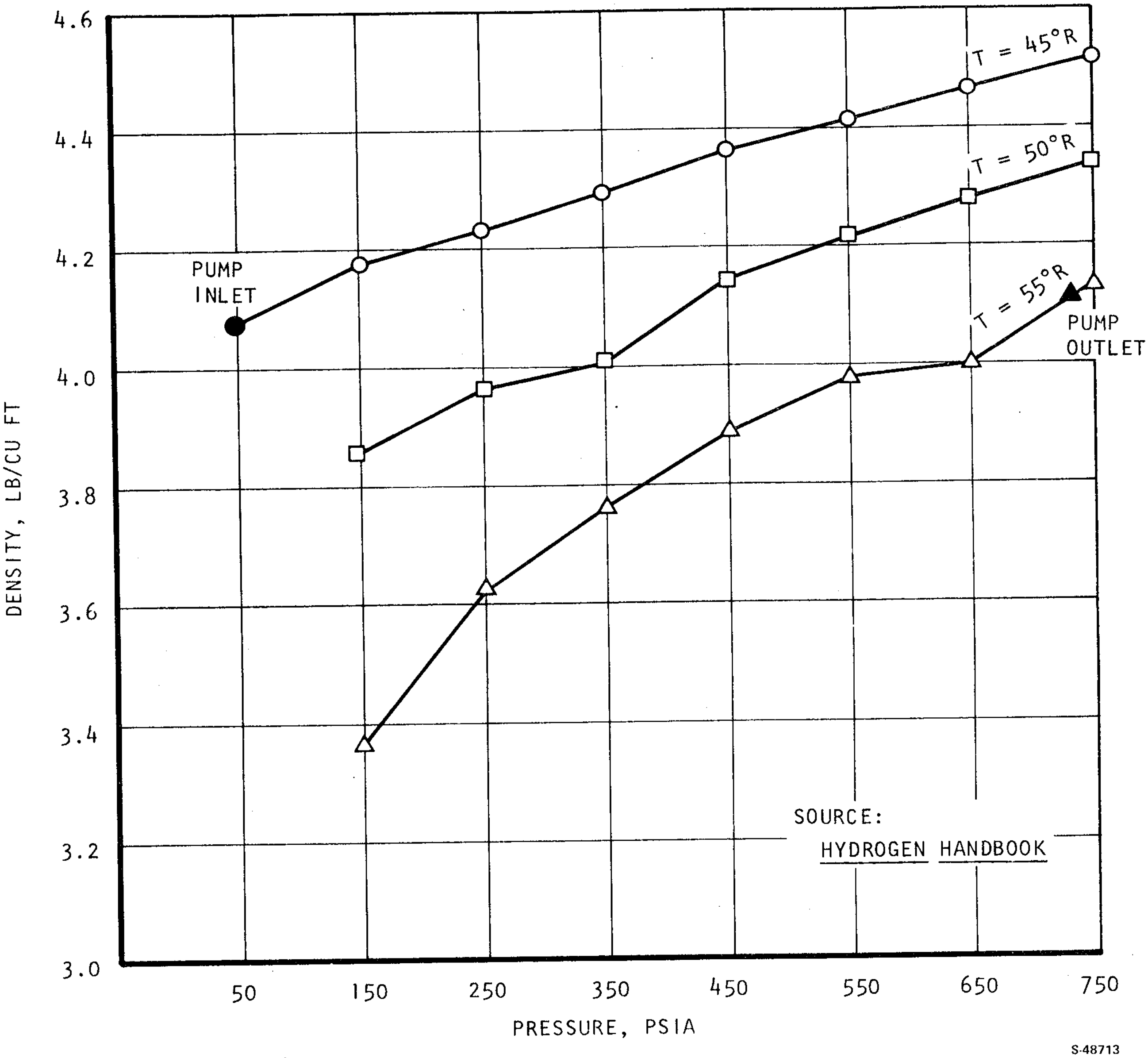


Figure 2-2. Density vs Pressure for Hydrogen

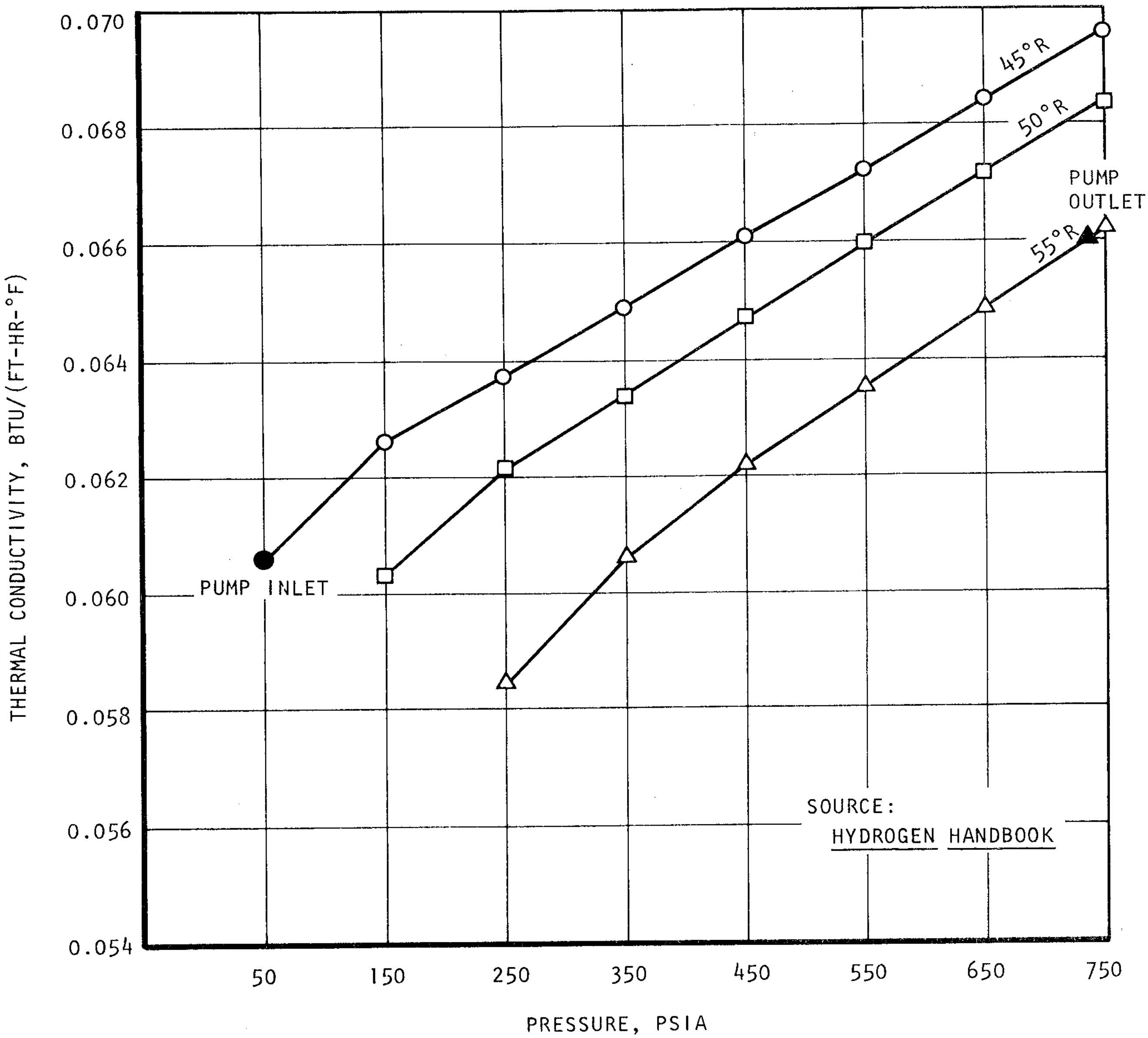


Figure 2-3. Thermal Conductivity vs Pressure for Hydrogen

S-48712

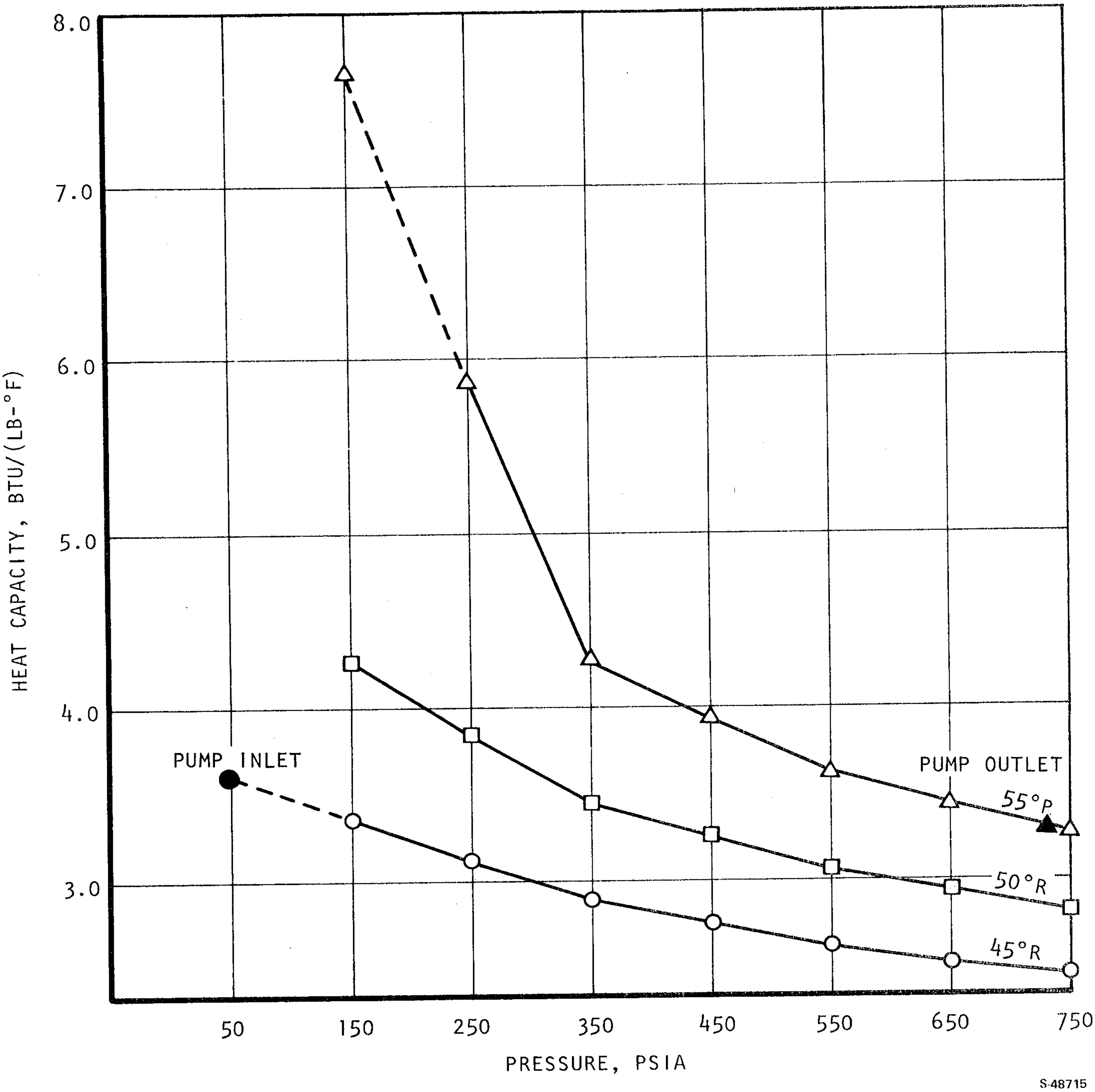


Figure 2-4. Heat Capacity vs Pressure for Hydrogen

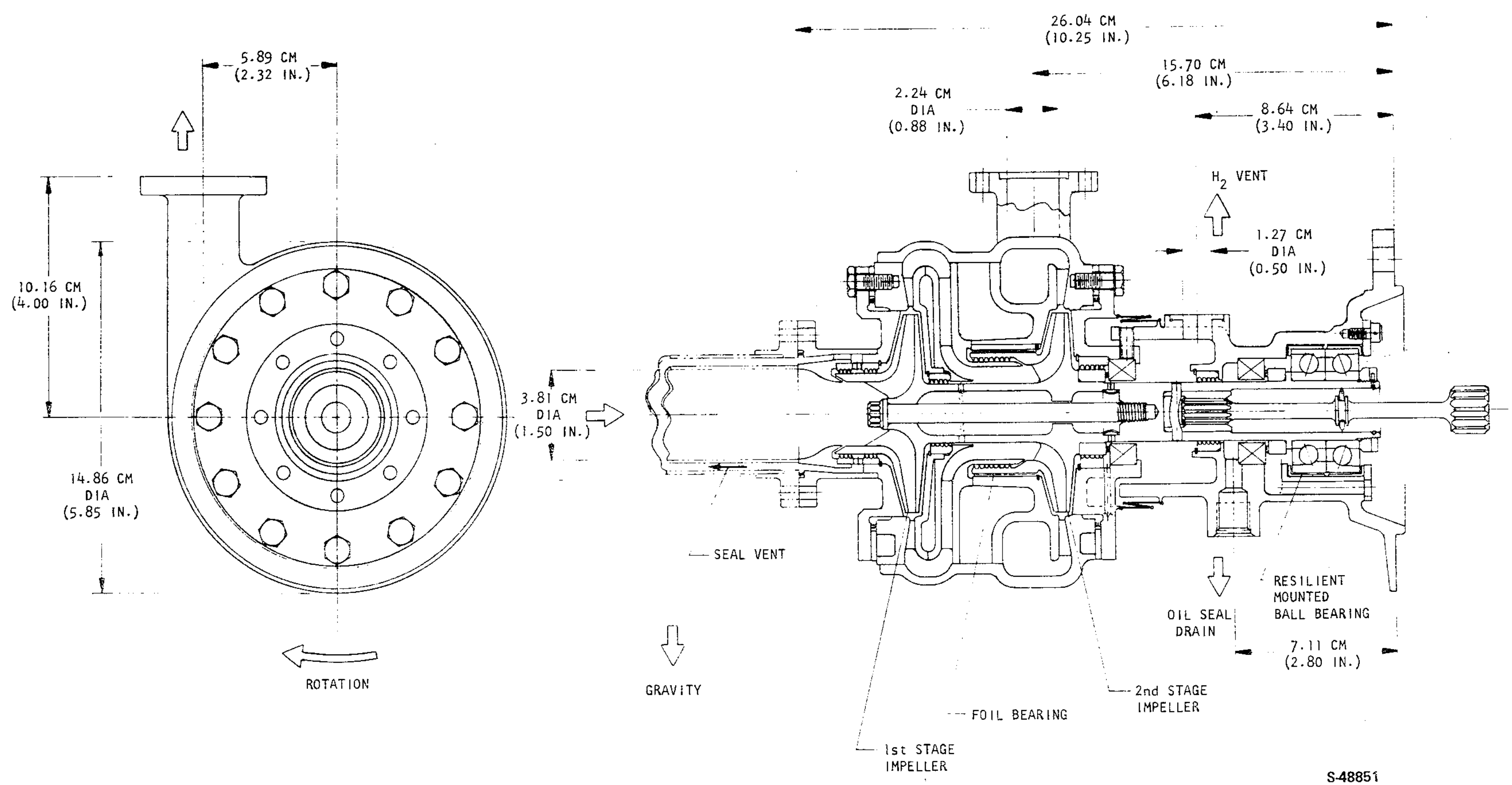


Figure 2-5. Engine High-Pressure $LH_2$ Pump

$\Omega$ = the gyroscopic rate

$r_e$ = the effective moment arm

Assuming a rotor polar inertia of $5.7 \times 10^{-4}$ lb-in.-sec$^2$, a gyroscopic rate of 0.5 rad/sec, and an effective moment arm of 3 in., the gyroscopic load is 0.5 lb, based on a rotor speed of 50,000 rpm. This load is much smaller than the hydraulic unbalance load.

The estimated unbalance is 48 lb at the operating speed of 50,000 rpm. This appears much larger than the first two load components. However, the effective load the bearing experiences will depend on the ratio of the natural frequency to the shaft speed and also on the degree of damping.

Letting $P_o$ be the unbalance force, k the effective bearing stiffness, and C the effective bearing damping, the maximum transmitted bearing load is

$$W_u = k X_o \sqrt{1 + 4 \zeta^2 \left(\frac{\omega}{\omega_n}\right)^2} \tag{2-3}$$

where $\omega_n$ is the natural frequency,

$$\omega_n = \sqrt{\frac{k}{m_r}} = \sqrt{\frac{k g}{W_r}} \tag{2-4}$$

and $\zeta$ is the damping factor,

$$\zeta = \frac{C}{2\sqrt{k m_r}} \tag{2-5}$$

In the above, $m_r$ is the rotor mass, g is the gravity factor, and $X_o$ is the amplitude due to the unbalance force. $X_o$ is given by

$$X_o = \frac{P_o}{k} \frac{1}{\sqrt{\left[1 - \left(\frac{\omega}{\omega_n}\right)^2\right]^2 + 4\zeta^2 \left(\frac{\omega}{\omega_n}\right)^2}} \tag{2-6}$$

It can be seen from equations (2-3) and (2-6) that the effective bearing load gets smaller as the frequency ratio becomes much larger than unity.

Based on our foil journal bearing spring rate data, the frequency ratio is plotted in Figure 2-6 as a function of bearing diameter for three L/D (length to diameter) ratios: 0.5, 1, and 1.5. The corresponding unbalance amplitude and total bearing load (see equation (1-1)) are shown in Figures 2-7 and 2-8, respectively. A damping factor of 0.1 was used in the computation.

Our foil bearing data indicate a damping factor of about 0.1 to 0.15. Because there are no data on the interleaf Coulomb friction in an $H_2$ environment, it is not certain what the actual damping factor is for foil bearings operating in an $LH_2$ pump. For this reason, a low value of 0.1 was used. Moreover, it will be shown later that the bearing load and unbalance amplitude are insensitive to damping factor in the bearing size range of interest.

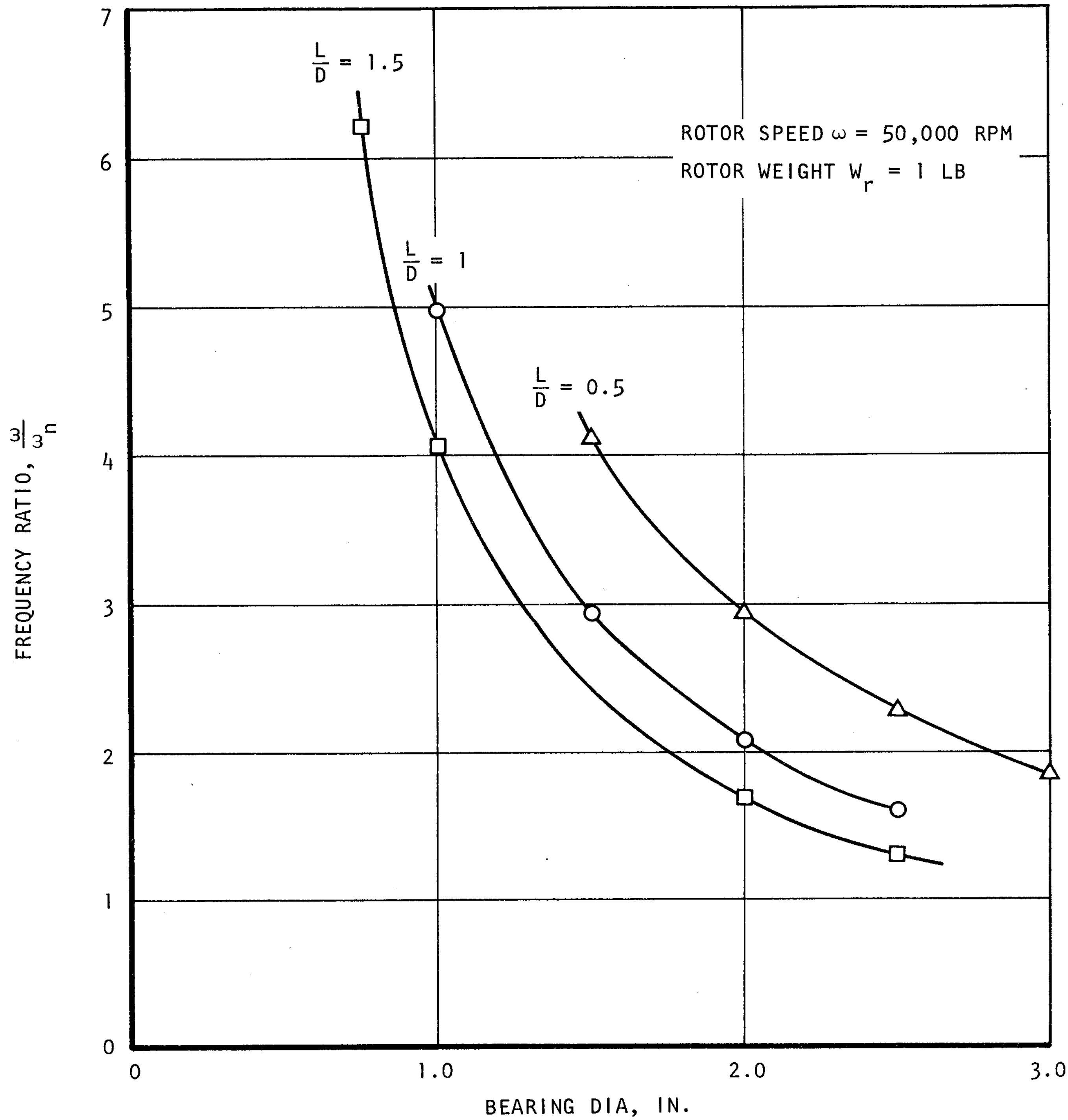


Figure 2-6. Frequency Ratio vs Bearing Size

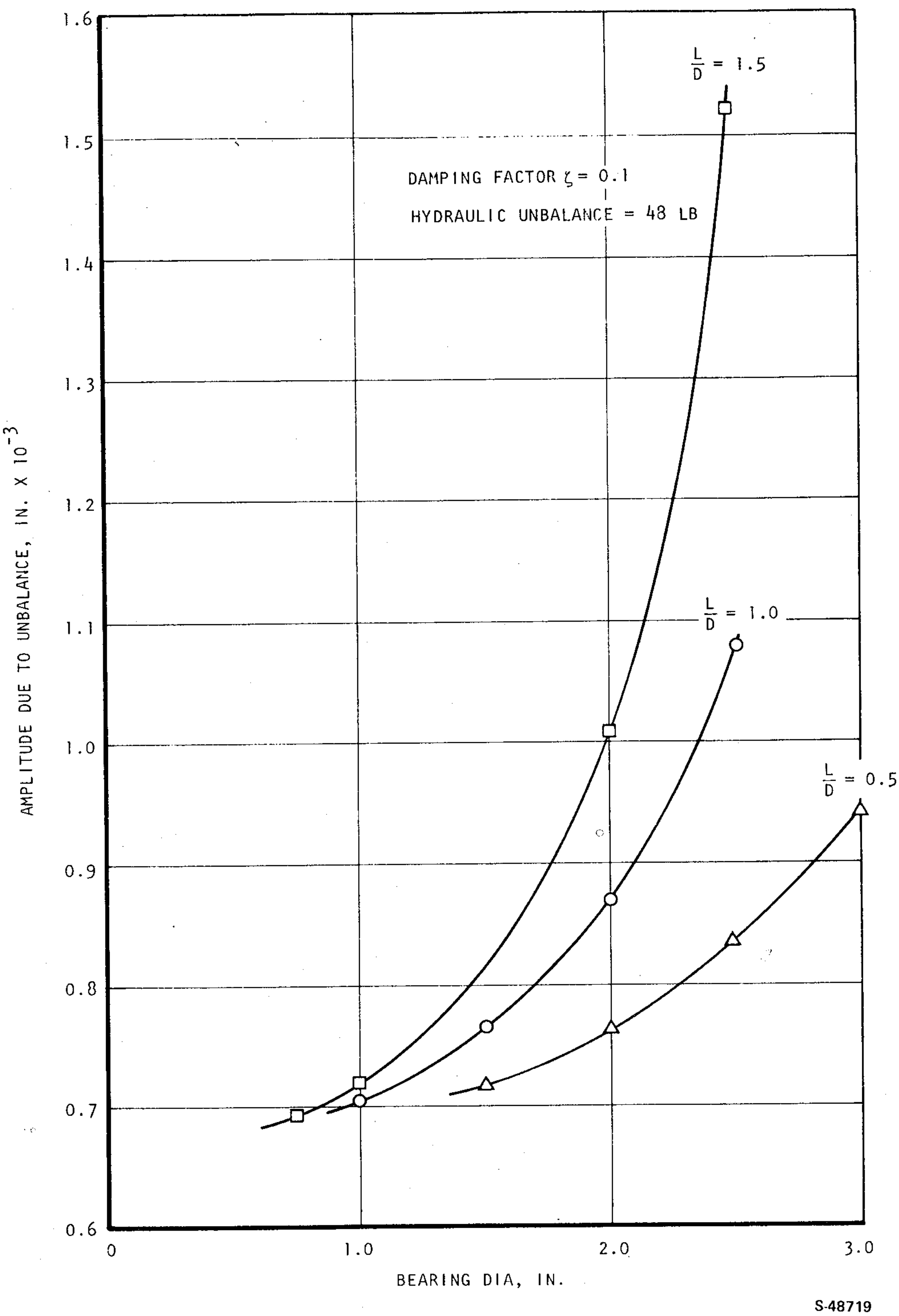


Figure 2-7. Unbalance Amplitude vs Bearing Size

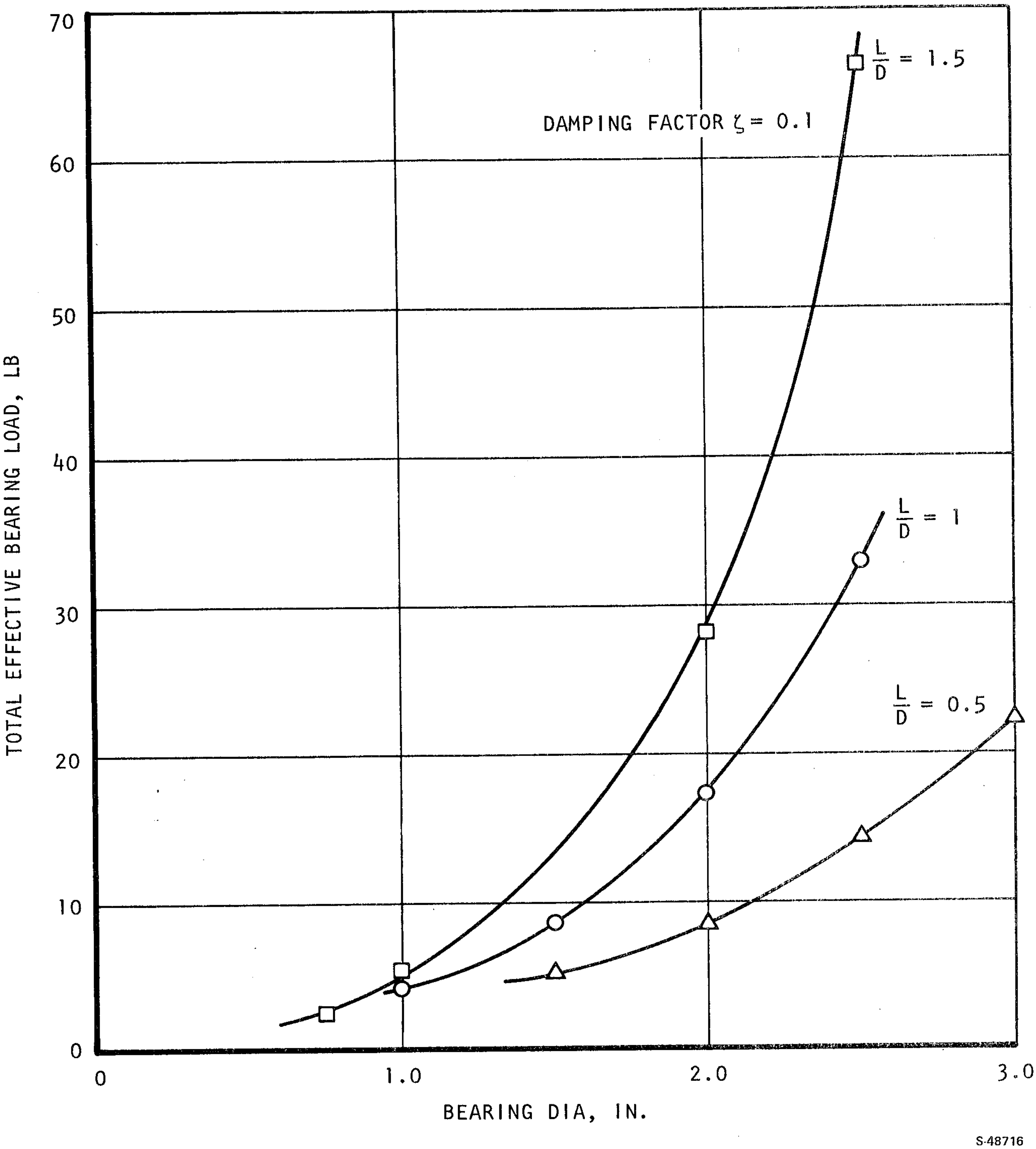


Figure 2-8. Total Bearing Load vs Bearing Size

Specific load vs bearing size is shown in Figure 2-9. The graph indicates a specific bearing load of 4 ~ 5 psi in the size range of interest.

## 2.2.2 Preliminary Sizing

In the normal pump operating condition (~50°R and 50 to 750 psia), $H_2$ behaves more like an incompressible fluid in its density and viscosity variations. Our bearing load capacity data were obtained mainly by using air as the lubricant. Although air is compressible, it will be conservative to use the air load capacity data to size the bearing to be operated in the $LH_2$ pump under identical speed and viscosity conditions.

For incompressible fluids, the bearing load capacity will be roughly proportional to speed and viscosity. Under this approximation, Table 2-1 shows the minimum load capacity of three AiResearch foil journal bearings operating in the $LH_2$ pump condition. It is seen that all of these bearings have ample load capacity.

Because of the high density of $H_2$ relative to air, the Reynolds number of an $LH_2$ pump bearing is high. For example, the Reynolds number based on a film thickness of 0.0005 in. is about 9,500 for a 1.75-in.-size bearing. This high Reynolds number turbulence effect will further enhance the load capacity of the bearing at the expense of high power loss.

TABLE 2-1

$LH_2$ PUMP FOIL BEARING
MINIMUM LOAD CAPACITY

| | Bearing Size, in. | | |
|---|---|---|---|
| | 0.85 | 1.75 | 3.00 |
| Test condition in air | | | |
| Speed, rpm | 60,000 | 47,500 | 25,000 |
| Viscosity, $10^{-9}$ lb-sec/sq in. | 2.66 | 2.66 | 2.66 |
| Observed load,* psi | 15 | 25 | 22 |
| $LH_2$ pump condition** | | | |
| Speed, rpm | 50,000 | 50,000 | 50,000 |
| Viscosity, $10^{-9}$ lb-sec/sq in. | 1.48 | 1.48 | 1.48 |
| Minimum load capacity, psi | 7.0 | 15 | 25 |

*Not the ultimate load capacity; rather, the attained load capacity
**50°R and 450 psia

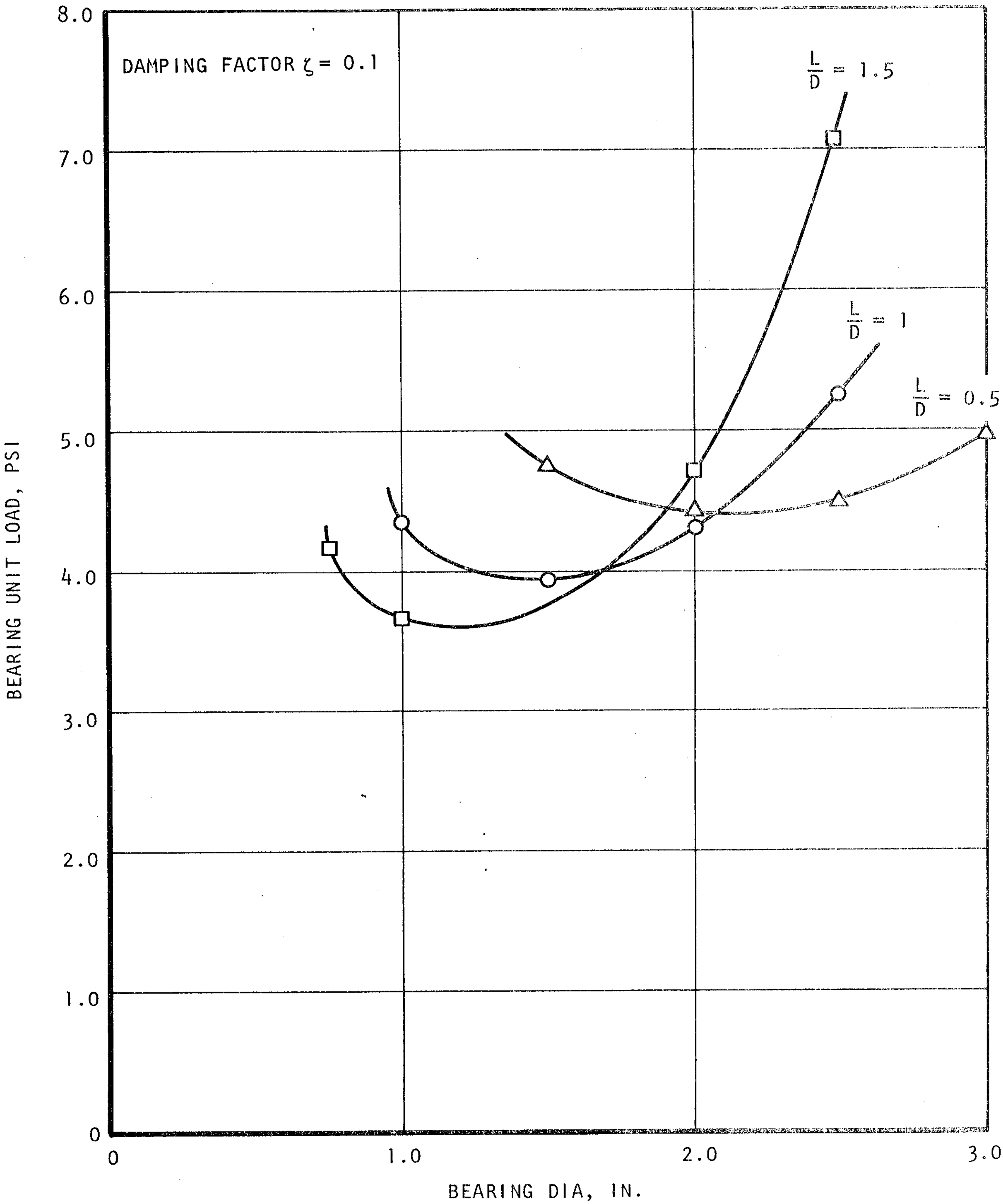


Figure 2-9. Specific Bearing Load vs Bearing Size

Although bearings as small as an 0.85-in. size appear to have adequate load capacity, they are susceptible to buzzing instability during starts. This is because the natural (resonant) frequencies of small bearings are lower than their full-film speeds, i.e., the minimum speeds at which the hydrodynamic film is fully developed.

The natural frequency versus bearing size is shown in Figure 2-10. Also given in the figure are the full-film speed lines for several surface roughness combinations. These full-film speed lines were obtained by a computerized calculation in which bearing minimum film thickness was computed as a function of shaft speed. The full-film condition was assumed to have established when the minimum film thickness was four times the combined surface roughness:

$$\sigma = \sqrt{\sigma_1^2 + \sigma_2^2} \tag{2-7}$$

where $\sigma$ is the combined surface roughness, and $\sigma_1$ and $\sigma_2$ are the roughnesses of the two opposing surfaces.

The calculated full-film speeds as functions of bearing size shown in Figure 2-10 are for three values of combined roughness: 10, 17, and 30 $\times 10^{-6}$ in. The medium value of 17 $\times 10^{-6}$ in. is typical for the combination of Teflon S coated foil bearing and thin, dense, $C_r$-plated shaft surface that is used in most of the AiResearch foil-bearing turbomachines.

It appears from Figure 2-10 that a bearing size of 2 in. is a reasonable choice for the preliminary pump design. For an L/D ratio of 1, this bearing should have at least 15-psi load capacity, based on the data in Table 2-1.

Figure 2-10 also indicates that, if necessary, the full-film speed can be lowered by decreasing the surface roughnesses.

As mentioned earlier, the effects of bearing damping on unbalance vibration amplitude and bearing load are small. This is illustrated in Figure 2-11, in which the unbalance amplitude is shown for three values of damping factor (0.05, 0.1, and 0.15).

### 2.2.3 Power Loss

The power losses for foil bearings to be used in an $LH_2$ pump were estimated. Computerized analyses were employed to perform the calculations, which include the effects of speed, fluid viscosity, and bearing geometry. The turbulence effect* due to a high bearing Reynolds number was also considered. The transition from laminar to turbulent flow was assumed to take place at a Reynolds number of 2000.

The operating condition for the preliminary pump design reported in NASA CR-145369 was used in the power loss calculation. The speed was 50,000 rpm, and the fluid viscosity was 1.48 $\times 10^{-9}$ lb-sec/sq in. (50°R and 450 psia).

---

*D.F. Wilcock, "Turbulent Lubrication--Its Genesis and Role in Modern Design," Journal of Lubrication Technology, Vol. 2, January 1974, pp. 2.

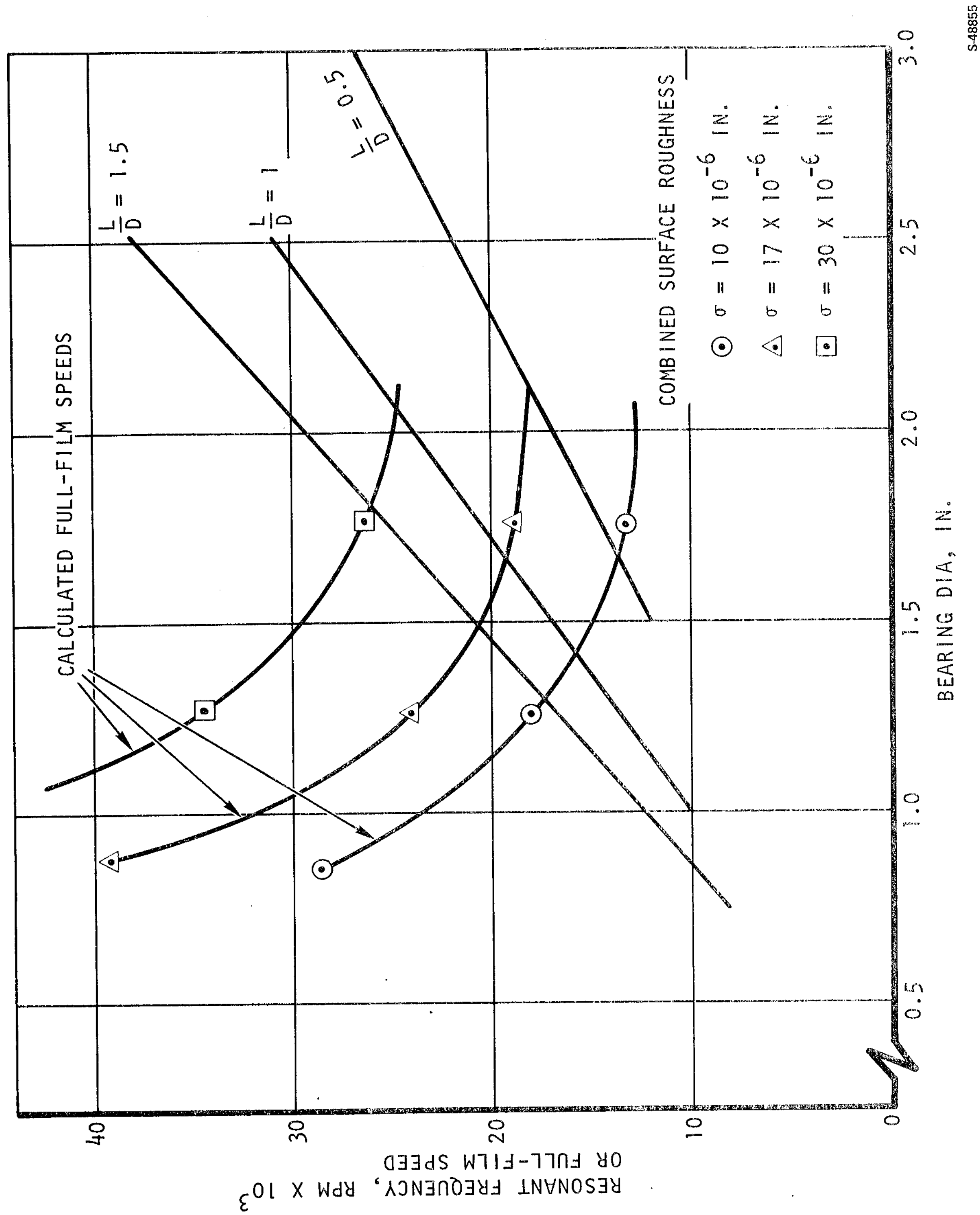


Figure 2-10. Natural Frequency vs Bearing Size

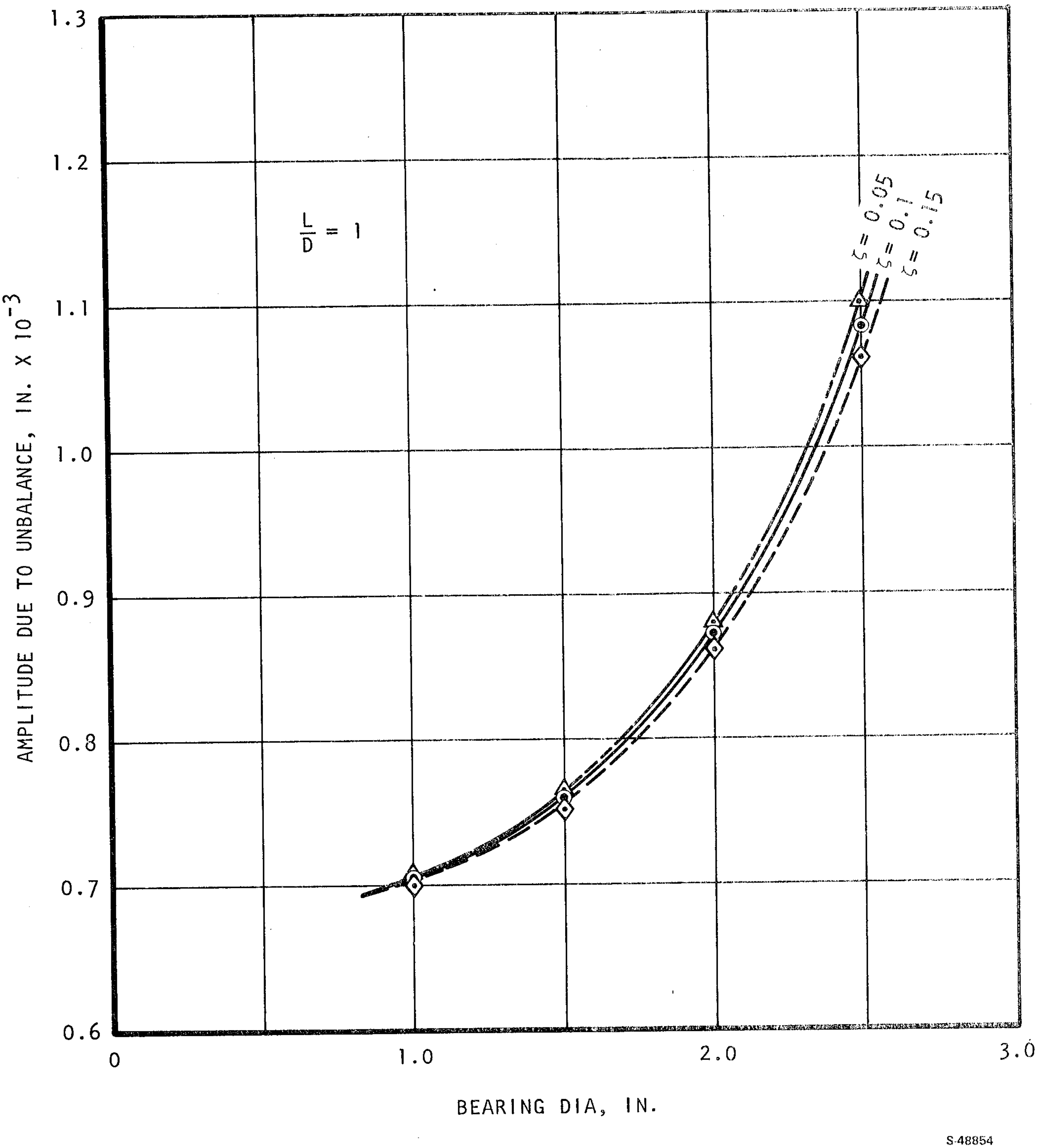


Figure 2-11. Effect of Damping Factor

The journal bearing loss is plotted in Figure 2-12 as a function of bearing diameter for three values of the L/D ratio (0.5, 1., and 1.5). The dotted lines are power loss curves, excluding any turbulent effect. Note that for a 2 in. by 2 in. bearing, the power loss at the design point condition is 154 w.

## 2.3 THRUST BEARINGS

### 2.3.1 Thrust Bearing Load

The axial thrust load results mainly from hydraulic unbalance, and the magnitude of this force can be controlled by proper balancing techniques. For the preliminary pump design reported in NASA CR-145369, it is established that the thrust load can be limited to 10 lb.

### 2.3.2 Preliminary Sizing

To determine the load capacity of foil thrust bearings operating in an $LH_2$ pump environment, a procedure similar to that for sizing foil journal bearings was used.

Table 2-2 presents the attained load capacity in air of four AiResearch foil thrust bearings ranging in size from 1.68 to 4.24 in. These load data were scaled by the viscosity and speed ratios to obtain the minimum load capacity of the foil bearings operating at $LH_2$ pump conditions (see the lower portion of the same table).

As mentioned earlier, it is conservative to scale the load data tested in air to obtain the minimum load capacity for the $LH_2$ pump application because of the incompressible characteristic of $H_2$ under normal pump operating conditions (50°R and 50 to 750 psia). Moreover, the turbulence effect due to a high bearing Reynolds number (15,000 for the 3.80-in.-OD bearing based on a 0.0005-in. film thickness) will further enhance the bearing load capacity.

It may be seen from Table 2-2 that even a 1.68-in.-OD bearing will have sufficient load capacity for the $LH_2$ pump application. The actual size of the thrust bearing will be determined in part by the rotor-bearing configuration. If the thrust bearing is an integral part of a total journal and thrust bearing system, as for most foil-bearing-supported turbomachines, the inside diameter of the thrust bearing is usually determined by the journal bearing diameter.

The preliminary pump design shown in Figure 2-5 utilizes a foil journal bearing in the "cold end" between two compressor impellers and a duplex ball bearing pair sufficiently away from the cold pump to take the thrust load. A separate double-acting foil thrust bearing can be placed near one of the impellers to take the thrust unbalance if so desired. An alternate and more practical arrangement will be a total foil bearing system consisting of two journal bearings and a double-acting thrust bearing in between, an arrangement that eliminates the duplex ball bearing pair. It was mentioned earlier that journal bearing size would be around 1.75 to 2 in. for the preliminary

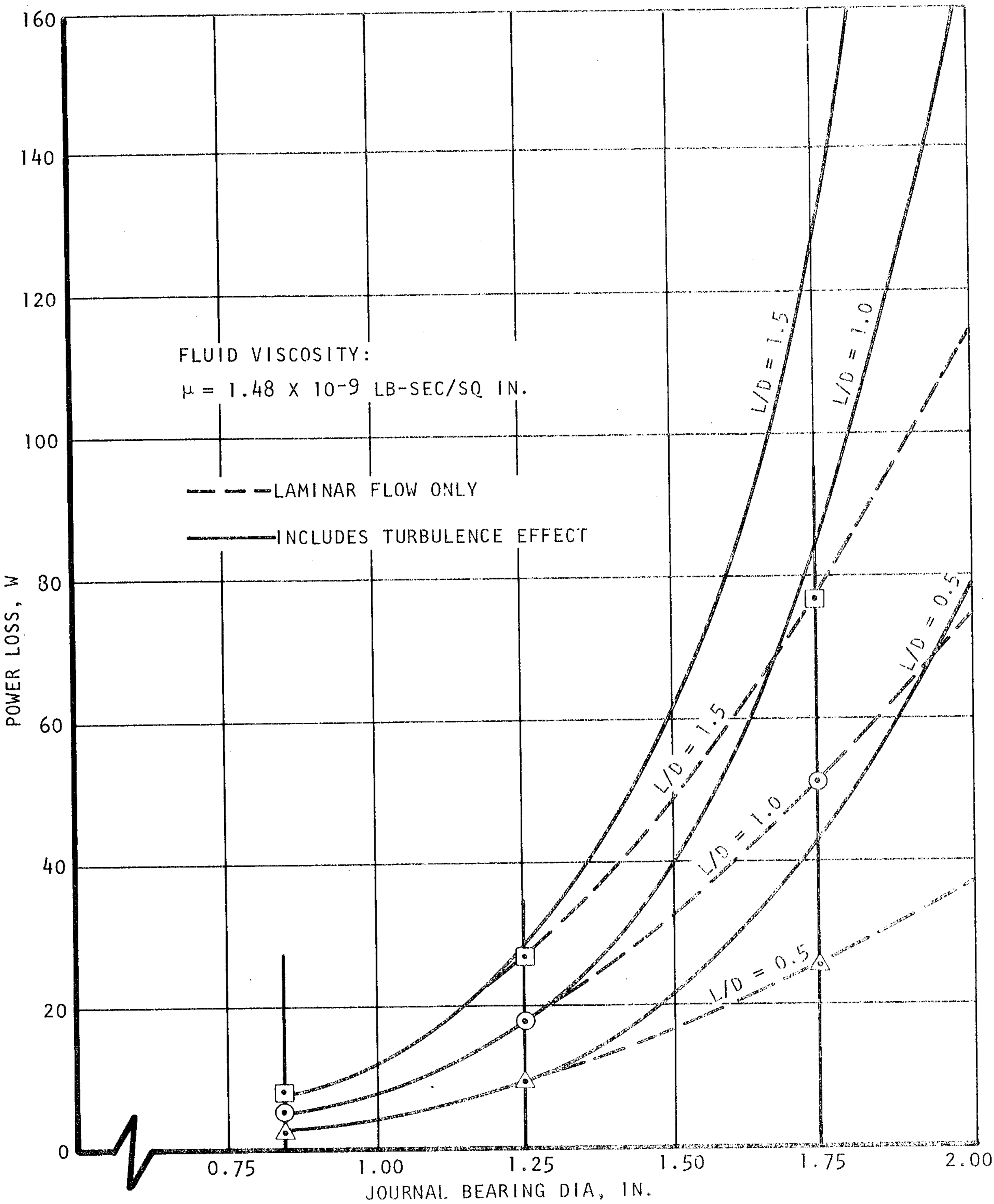


Figure 2-12. Journal Bearing Power Loss

TABLE 2-2

$LH_2$ PUMP FOIL THRUST BEARING
MINIMUM LOAD CAPACITY
COMPARED TO TEST DATA IN AIR
(four different sizes)

| | | | | |
|---|---|---|---|---|
| Bearing size | | | | |
| OD, in. | 1.68 | 2.79 | 3.80 | 4.24 |
| ID, in. | 0.93 | 1.40 | 1.95 | 2.35 |
| Area, sq in. | 1.53 | 4.56 | 8.34 | 9.77 |
| Test condition in air | | | | |
| Speed, rpm | 48,000 | 42,000 | 40,000 | 30,000 |
| Viscosity, $10^{-9}$ lb-sec/sq in. | 2.66 | 2.66 | 2.66 | 2.66 |
| Observed load capacity,* psi | 20 | 22 | 21 | 21 |
| $LH_2$ pump condition** | | | | |
| Speed, rpm | 50,000 | 50,000 | 50,000 | 50,000 |
| Viscosity, $10^{-9}$ lb-sec/sq in. | 1.48 | 1.48 | 1.48 | 1.48 |
| Minimum load capacity, psi | 12 | 15 | 15 | 19 |
| Minimum total load, lb | 18.4 | 68.4 | 125.1 | 185.6 |

*Not the ultimate load capacity; rather, the attained load capacity
**50°R and 450 psia

pump design. Then the thrust bearing of size 1.95-in. ID and 3.80-in. OD would be a reasonable choice. According to Table 2-2, the load capacity at the pump design condition is 125 lb.

The full-film speed (the minimum speed at which the hydrodynamic film is fully developed) of a thrust bearing is in general lower than that of a journal bearing of similar size. Therefore, there should be no buzzing instability associated with the rotor radial resonance during starts. The stiffness of a thrust bearing can be made sufficiently large, so that the axial resonant frequency is higher than all full-film speeds.

### 2.3.3 Power Loss

The power loss for thrust bearings was computed using an established computer program. The turbulence effect due to a high bearing Reynolds number was included. The speed used was 50,000 rpm, and fluid viscosity was 1.48 x $10^{-9}$ lb-sec/sq in.

Figure 2-13 presents the power loss for foil thrust bearings. Again, the dotted line is the power loss based on laminar flow. For a 3.80-in.-OD thrust bearing, the power loss is 280 w at the design condition.

## 2.4 FEASIBILITY OF FOIL BEARING COATING

The bearing segments of foil bearings need protective coating to withstand the wear during starts and stops and to lower the friction for easy starts. The Teflon S coatings have been used successfully for almost all AiResearch foil-bearing-supported turbomachines presently in operation. All these machines operate in above-room-temperature environments. Whether the Teflon S coatings will work properly in the 50°R $LH_2$ pump design condition requires direct rig tests. Two recent development tests performed at AiResearch have offered very promising results:

(a) Teflon S coated foil journal bearings have been tested successfully down to 160°R in a turbo-expander application using $GN_2$.

(b) The Teflon S coated foil segments have successfully passed the static thermal cycle tests. In the tests, the specimens were dipped into an $LN_2$ container (139.2°R) 10 times at 25-min intervals (10 min in $LN_2$ tank and 15 min in room environment). Neither cracking nor curvature change was observed.

The above results make it reasonable to assume that the Teflon S coatings would work for the $LH_2$ pump application.

## 2.5 CONCLUSIONS ON FEASIBILITY OF THE FOIL BEARING APPLICATION

This Phase I analytical study indicates that foil bearings, journal bearings as well as thrust bearings, are feasible for the $LH_2$ pump application.

In the study, the effects of the low viscosity and incompressibility of $H_2$ at the normal pump operating condition were considered in performing the preliminary sizing of both journal and thrust bearings.

The major load component for the journal bearing was the synchronous hydraulic radial unbalance that occurs at the minimum off-design pump flow. Reasonable size foil journal bearings were found to have ample load capacity to take this unbalance load plus the rotor weight and gyroscopic maneuver load.

In addition to the load capacity, the problem of buzzing during starts was considered. To be free from this instability, the natural frequency of the bearing-rotor system must be larger than the bearing full-film speed. This requirement determines a minimum bearing size. For the preliminary pump

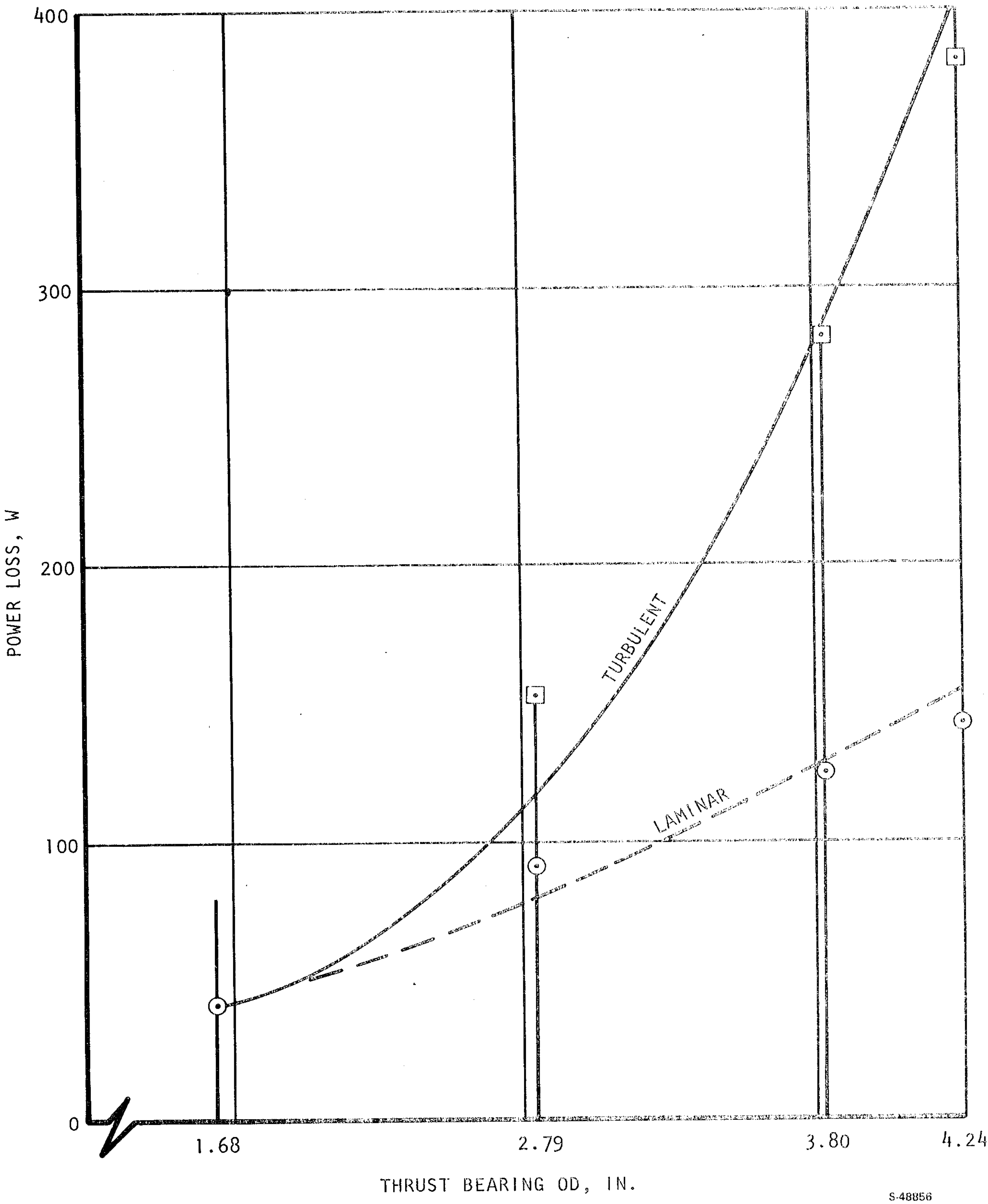


Figure 2-13. Thrust Bearing Power Loss

design reported in the referenced NASA report, it was found that a 2 in. by 2 in. foil journal bearing would be a reasonable choice satisfying both the load capacity and stability requirements.

Foil thrust bearings can be placed near one of the impellers to take the thrust unbalance (refer to the preliminary pump design, Figure 2-5). Or they can be used in conjunction with the foil journal bearings to form a total foil bearing system. It was found in this study that reasonable size thrust bearings would have adequate load capacity with respect to axial thrust unbalance.

The full-film speed of a thrust bearing is in general lower than that of a journal bearing of similar size. Therefore, there should be no buzzing instability associated with the rotor radial resonance during starts. The stiffness of a thrust bearing can be made sufficiently large, so that the axial resonant frequency is higher than all full-film speeds.

In conjunction with the 2 in. by 2 in. journal bearings selected for the preliminary pump design, a thrust bearing of size 1.95-in. ID and 3.80-in. OD would be a reasonable choice.

The Teflon S coatings used on foil segments to withstand wear during starts and stops and to lower the friction for easy starts appear very promising for the $LH_2$ application. This is based on the results of cryogenic compatibility tests performed recently at AiResearch.

## 3. PROPOSED TEST PROGRAMS

### 3.1 DEFINITION OF BEARING LOADS

To define the bearing static and dynamic loads with more confidence, a test program is proposed that will use an existing pump, AiResearch PN 580950, as the test article. The present carbon-graphite bearings will be replaced by ball bearings supported by mounts with strain gages attached. Tests will be run on water at the following conditions:

| Condition | Value |
|---|---|
| Flow rate, gpm | 0 to 70 |
| Pressure rise, psig | 170 to 200 |
| Speed, rpm | 11,500 |

A comparison of the impeller dimensions for the AiResearch PN 580950 pump with those of the $LH_2$ pump listed in CR-145369 is given below:

| Impeller Dimension | $LH_2$ Pump | AiResearch Pump |
|---|---|---|
| Diameter, in. | 3.730 | 3.180 |
| Eye diameter, in. | 0.985 | 1.36 |
| Tip width, in. | 0.055 | 0.105 |

It is recognized that the test program proposed will operate at a Reynolds number on an order of magnitude less than that for the $LH_2$ pump, but because bearing loads are primarily associated with pressure rise, the test should produce reasonably accurate data at a modest cost.

### 3.2 BEARING BENCH TESTS

Analyses performed so far have shown very promising results for the application of foil bearings to $LH_2$ pumps. Direct bench tests are the logical next step to verifying totally the applicability of foil bearings in an $LH_2$ pump system. These tests constitute the proposed Phase II program.

Preliminary consideration has been given to the Phase II program. A bearing test rig totally supported by foil bearings--similar to AiResearch foil journal bearing rigs--appears suitable for $LH_2$ pump foil bearing evaluation tests. Figure 3-1 presents a schematic of the proposed test rig. A

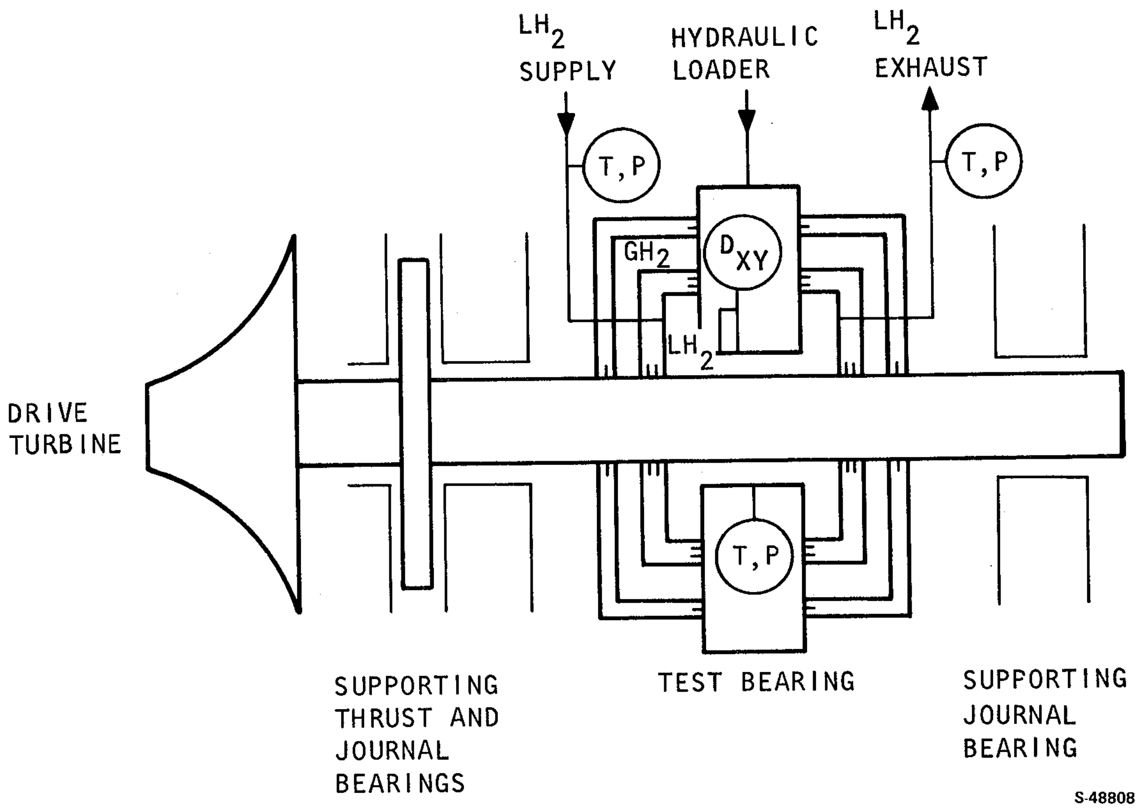


Figure 3-1. $LH_2$ Foil Bearing Test Rig

drive turbine is supported by a pair of foil journal bearings and a double-acting foil thrust bearing. The test bearing is situated in the midsection. The test bearing housing is enclosed by two chambers. The inner chamber, which totally contains the test bearing, is filled with $H_2$ at the typical $LH_2$ pump condition (~50°R and ~450 psia). The outer chamber contains low-temperature $GH_2$ at some intermediate pressure level to insulate the cold inner test section and to reduce the leakage rate of the test fluid.

An external loader will provide loading to the test bearing. The temperature and pressure of the $H_2$ in the test chamber as well as the shaft motion in terms of proximity probes will be controlled and recorded.

The $H_2$ supply loop system is shown schematically in Figure 3-2. $H_2$ is provided from pressurized bottles. It first goes through a pressure reducing valve and is then pre-chilled in an $LN_2$ tank. The final test temperature is achieved by means of an $LH_2$ heat exchange bath. Safety burnoff stacks are provided in the loop. The bearing test rig setup is summarized in Figure 3-3.

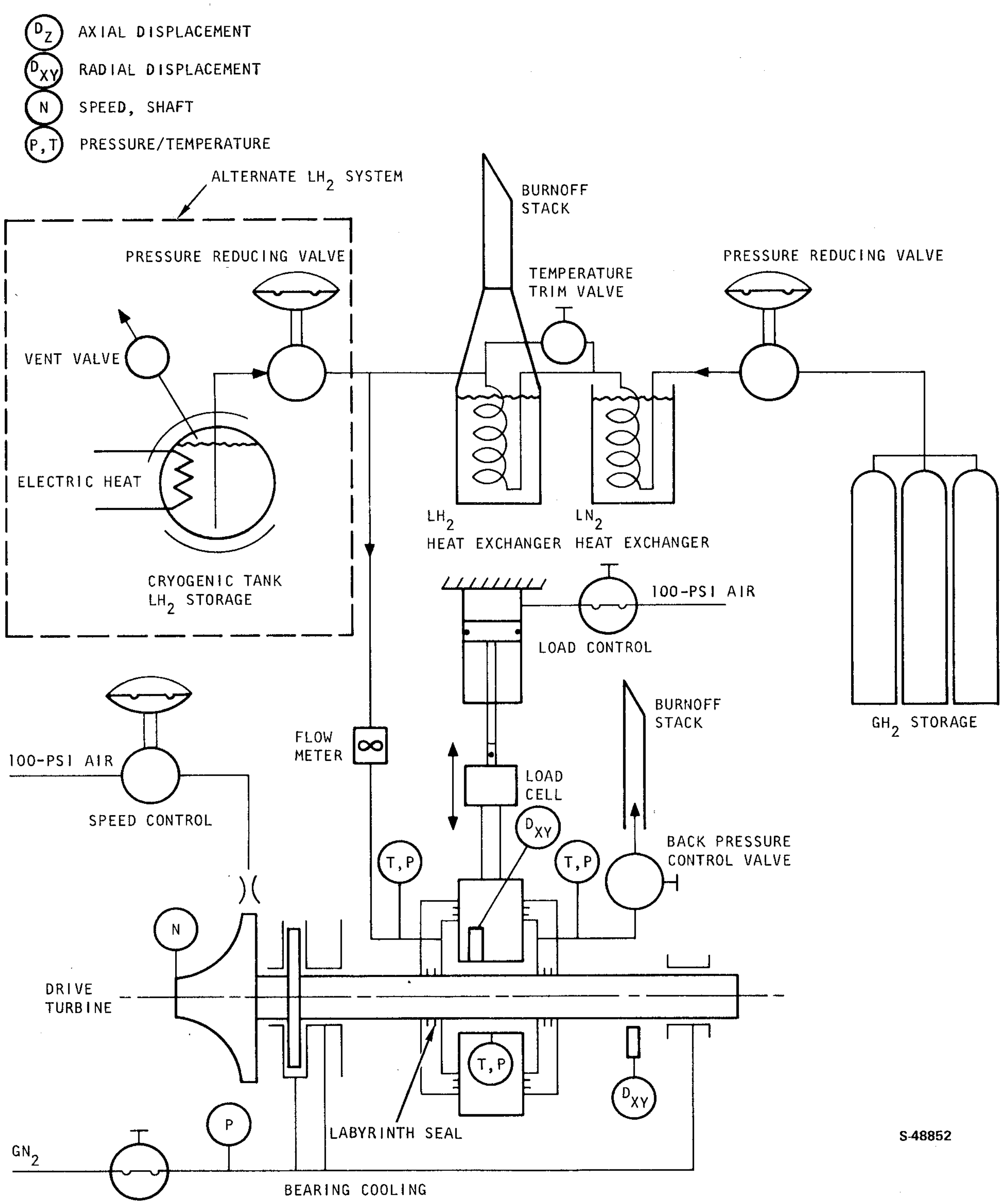


Figure 3-2. Schematic of $LH_2$ Bearing Test Setup

GARRETT

**TEST**

$LH_2$ BEARING TEST EVALUATION SETUP

PREPARED BY: KND

PART NO. —

DATE: 1-30-80

**OBJECTIVE**

TO DETERMINE THE OPERATING CHARACTERISTICS OF FOIL BEARINGS WHEN EXPOSED TO SUPERCRITICAL HYDROGEN AS THE FLUID MEDIUM

**FACILITY**

TORRANCE, CA.
SYSTEMS TEST LABORATORY

**SCHEMATIC**

SEE TEST SETUP SCHEMATIC, FIGURE 3-2.

**EQUIPMENT AND INSTRUMENTATION**

1. CRITICAL $H_2$ SUPPLY SYSTEM
2. TURBO DRIVE BEARING FIXTURE
3. RADIAL LOAD CONTROL
4. SHAFT DISPLACEMENT MEASURING SYSTEM
5. CONTROL AND INSTRUMENTATION CONSOLE
6. SAFETY BURNOFF STACKS

**PROCEDURE**

REGULATE THE DESIRED BEARING PRESSURE FROM THE SUPPLY OF $GH_2$. PRE-CHILL THE $GH_2$ TO 140°R WITH $LN_2$, FINAL-CHILL, AND TRIM WITH THE $LH_2$ BATH TO 50°R. ADJUST BACK PRESSURE VALVE FOR 5 PSID ACROSS FOILS. ACCELERATE TURBINE TO 50,000 RPM. VARY RADIAL LOAD ON THE FOIL BEARING FROM 0 TO 20 LB. RECORD TEST DATA.

**REQUIRED DATA**

HYDROGEN FLOW RATE; TURBINE SPEED; FLUID AND BEARING TEMPERATURES, PRESSURES; SHAFT DISPLACEMENT X, Y, Z; AND FOIL HOLDER DISPLACEMENT RELATIVE TO SHAFT.

**ACCEPT/REJECT CRITERIA**

MUST MEET DESIGN REQUIREMENTS.

**NOTES**

CRYOGENIC TANK MAY BE USED AS THE CRITICAL HYDROGEN SUPPLY SYSTEM AS AN ALTERNATIVE.

S-48853

Figure 3-3. $LH_2$ Bearing Test Summary